

Transient analysis of individual return temperatures in hydronic floor heating systems

Simon Thorsteinsson^a, Henrik Lund Stærmosé^b, Jan Dimon Bendtsen^a

^a Section of Automation and Control, Department of Electronic Systems, Aalborg University, Denmark, sith@es.aau.dk.

^b Neogrid Technologies ApS, Niels Jernes Vej 10 - 9220 Aalborg east, Denmark, hls@neogrid.dk.

Abstract. In this work, we investigate some potential benefits and opportunities gained from monitoring the return temperature of all the circuits in a *hydronic floor heating* (FH) system. It is for example possible to obtain information on the flow distribution in the FH system. Since flow sensors are relatively expensive, most currently installed FH systems do not provide any information on the flow entering the forward manifold, let alone flows in the individual circuits. This lack of information inhibits analysis of performance and prevents commissioning of more advanced control methods. The approach proposed here, based on temperature sensors mounted on the exterior of the pipes, provides a possible cheap alternative to measuring the flows directly. Further, we argue that this retrofitted solution can be applied to most already installed floor heating systems. The paper contains a description of the retrofit kit and a dynamic model, which is shown to be able to replicate the behaviour of measurements acquired from an actual FH system installed in a single-family house, as well as a method for calculating the relative flows. The results show that flow-related parameters such as circulation time are, under the right circumstances, directly observable in the data. Overall, we conclude that measuring the individual return temperatures provides valuable information when monitoring the health and performance of a floor heating system.

Keywords. Floor Heating, Flow, Retro-fit, Estimation, Simulation

DOI: <https://doi.org/10.34641/clima.2022.140>

1. Introduction

In this paper we discuss the potential benefits of continuously measuring the return temperatures of the individual circuits in a *hydronic floor heating* (FH) system placed in a single family house, and propose a method to roughly estimate the *flow distribution* (FD) and thereby the distribution of energy consumption in the different FH pipes. The word *distribution* signals that only a relative, and not an absolute, measure of the heat consumption of the individual circuits is obtained.

On the topic of energy efficiency, single family houses are interesting and problematic. Interesting because they cover a significant amount of heated area (about 55 % in Denmark) [1]. Problematic since this large share is distributed over many small units, which means the potential for energy savings in each unit is relatively small. Further, a majority of these units are owned by the residents themselves [2], meaning that any investment into energy efficiency has to be understood from a perspective of a relative low budget. The consequence is that, without any active incentive programs, energy

efficiency solutions for single family houses have to be highly cost effective. Solutions for retrofitting existing buildings are, in this text, characterized into two main groups, passive, where changes are made to the physics of the building, and active, which covers changes in the operation under the existing conditions. The active solutions to a large extent cover exchanging existing controllers, together with updating the set of sensors and actuators, in order to operate the overall system more efficiently.

Returning to the theme of this paper, a question arises: why is the FD, in a FH system, interesting and useful information? To answer this, it is helpful to visit a class of controllers called Model Based Controllers. Among controllers classified as model based, *Model Predictive Control* (MPC) is the most widely known. The method combines a model with an objective function, which assign costs to states and inputs over a control window. To obtain the specific model it has to be constructed and identified. In [3] the authors used a grey-model method called *Maximum Likelihood* (ML) to estimate the dynamics of an arctic low-energy house heated by FH. For the

identification of the parameters, the heat flow, based on forward/return temperature and mass flow of the water, is used as input for each circuit. A *Least Squares* (LS) method is used by [4] to fit the parameters in a grey-box model. In [5] the authors use an *Unscented Kalman Filter* (UKF) to online estimate the parameters of a five room building. Common for the mentioned texts is that they assume the heat flows from the HVAC systems to be known. This is rarely the case in single family houses. The text in [5] touches upon this problem and discusses numerical instabilities, related to not providing a scaled input for the different rooms. Although, the scale here refers to the difference of actual heat flows between individual rooms, we argue that on room level a relative scale based on e.g. FD is enough, since it is possible to further scale the relative estimates, if a central measure of the heat consumption is available. This is e.g. the case if the house is provided by district heating, since the overall heat consumption is needed to settle the energy bill. The authors of [3] do something similar when they correct the individual estimated heat flows according to the measured total heat consumption obtained centrally. Further, being able to scale FH circuits is useful in MPC. If all circuits are considered equal the MPC cannot ration the energy appropriately. If the actual heat consumption of the rooms are not obtainable, then it is at least useful to know whether one circuit is twice as expensive as the other. The notion of flow distribution and relative heat distribution is not new, [6] defines it as *relative heating coefficient* (RHC). The authors derive and compare an array of RHCs, which are used to rate the heat efficiency of the rooms of an office building. The work carried out in [6] lays the foundation for the work of this paper. Having established the importance of knowing the flow distribution and relative heating distribution, we pose the hypothesis: *It is possible to obtain a relative flow and heating distribution, based on measuring the forward/return temperature and control-valve state for all circuits. This approach outperforms scaling circuits using only floor area distribution.*

The rest of the paper contains an introduction to the system and retrofit-kit. Sec. 2. describes a simulation, which is used to investigate the method under ideal circumstances, followed the experiment conducted in the test house. Section 3. contains results from the simulation and test house before Sec. 4. concludes.

2. Method

This section presents the retrofit kit, simulation and derivation for the relative heating coefficient.

2.1 System

Figure 1 presents the system which is considered in this paper. The system reflects a common installation seen in many single family houses. The heat source provides a common forward temperature for the FH circuits. Each floor heating circuit is ON/OFF controlled with hysteresis based on temperature difference between measured room temperature and reference. The actuators are wax-motor valves [7]. The mass flow in circuit j , q_j combined with the total flow entering the forward manifold q are considered unknown.

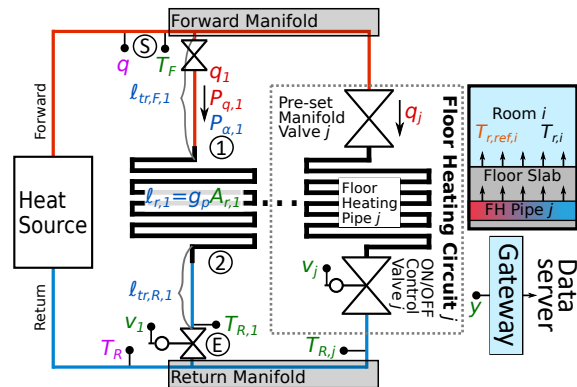


Fig. 1 – The system diagram containing the important signals. The signals are color coded: (green) measured signals or known inputs, (blue) estimated parameters, (magenta) measured for validation and (red) unknown but desired variables.

The FH system is placed in a test house, where data is gathered using the retrofit kit presented in the upcoming section. The house is built according to the BR2020 standard and heated using an air-to-water heat pump. There are 15 FH circuits distributed on two manifolds. The FH circuits are controlled using temperature feedback from the rooms. Each room has one thermostat. Rooms with more than one FH circuit are controlled using the same thermostat. Two rooms have two circuits, one has three, and the remaining have one each.

Assumption 1 (Constant flow). The flow in an open circuit is constant, regardless of the state of the other FH circuits.

Assumption 2 (Common cross-area). The cross area of the pipe A_p is the same for all FH circuits.

Assumption 3 (Measured return temperatures). The return temperature for each FH circuit is measured.

Assumption 4 (Common pipe length per m^2 floor). Pipe length per square meter floor, g_p , is the same for all rooms. This is shown in Fig. 1.

Assumption 5 (Floor area). The area covered by the floor heating pipe is assumed known.

We are aware that Assumptions 1, 2 and 4 are not always satisfied, but they are considered

acceptable in a retrofit situation. In the next section, we shall address a way to satisfy Assumption 3.

2.2 The retrofit kit

The retrofit kit, used to measure the return temperatures, consists of three components. Firstly, surface mounted temperature sensors are placed on each pipe before the collector manifold. The sensors, circled in red in Figure 2, are covered by insulation to lower effects from air temperature and heat radiation. The common forward temperature are measured in the same way. Second, the inputs to the ON/OFF control valves are monitored. The data samples are, in our case, sent via a gateway to an the online data server, provided by Neogrid Technologies ApS, but any sample-based data acquisition method may of course be employed. Third, the gateway supports overwriting control signals. Therefore, if the natural fluctuation of return temperatures is insufficient for estimation, reference manipulation is used to force control valves to open and close on demand.

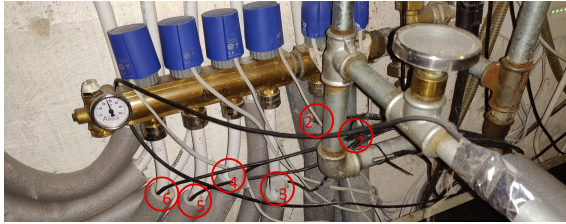


Fig. 2 – Shows temperature sensors placed under the insulation of each return pipe. Although the retrofit solution is the same, the picture is not from the test house discussed in this text.

2.3 Relative heat consumption

The heat consumption at time t for FH pipe j is in this text, defined as the instantaneous heat transferred from the water in the pipe to the floor. We denote this function as $\dot{Q}_{FH,j}(t)$. This heat transfer is dependent on multiple factors such as flow rate, temperature profile along the pipe and floor temperature, making it difficult to use in practice. To simplify the measure, the heat transferred is assumed well approximated by the difference between energy entering and exiting the pipe as seen in Eq. (1):

$$\dot{Q}_{FH,j}(t) \approx c_w q_j(t) (T_F(t) - T_{R,j}(t)) \quad (1)$$

With c_w being the heat capacity of water, T_F the forward temperature and $T_{R,j}$, q_j , the return temperature and mass flow of circuit j , respectively. The total heat consumption of the FH is given as the sum of the consumption of each circuit or as the total flow times temperature difference.

$$\dot{Q}_{FH} = \sum_{j=1}^N \dot{Q}_{FH,j}(t) = c_w q(t) (T_F(t) - T_R(t))$$

(2)

The return temperature, T_R , and total flow, q , are given as sums of contributions as well.

$$T_R(t) = \sum_{j=1}^N \frac{q_j(t)}{q(t)} T_{R,j}(t) \quad q(t) = \sum_{j=1}^N q_j(t) \quad (3)$$

As mentioned, both the total flow q and the circuit flows q_j are considered unknown, meaning that Eq. (2) cannot be computed in practice. Alternatively, as suggested in [6], one can introduce a *relative heating coefficient* (RHC) denoted β , which describes the relative consumption between the circuits. Instead of using the absolute flow a nominal distribution of flows is used. The term nominal distribution is used to indicate that the flow is a percentage share of the total and that the flows are independent of each other as stated in Assumption 1. The RHC derived in this test is seen in Eq. (4), and it is based on the advective heat flow of the circuit.

$$\beta_{q,j}(t) = v_j(t) \alpha_j (T_F(t) - T_{R,j}(t)) \quad (4)$$

Here, α_j is the flow distribution scalar and v_j binary valve state. The total relative consumption is given by Eq. (5).

$$\beta(t) = \sum_{j=1}^N \beta_j(t) \quad (5)$$

Eq. (4) is equivalent to Eq. (2) if Assumption 1 holds. The factor is $q_{\max} c_w$.

$$\dot{Q}_{FH} = q_{\max} c_w \beta_q \quad (6)$$

To get the by room percentage share of consumed heat, normalize the total heat transferred:

$$\mathcal{P}_{\beta,j}(\beta_j(t)) = \frac{\int_0^T \beta_j(t) dt}{\int_0^T \beta(t) dt} \quad (7)$$

The next section shows the derivation of the scalar α_j presented in Eq. (4)

2.4 Nominal flow distribution

We start by stating the two common flow equations for pipe with constant flow and pipe area.

$$q_j = v_j A_p \rho \quad (8)$$

$$v_j = \frac{\ell_{r,j}}{\Delta t_{r,j}} \quad (9)$$

where v is the velocity of the water, A_p is the area of the cross section of the pipe and ρ is the mass density of water, ℓ_r is the length of the pipe under the floor and Δt_r is the time water spends under the floor in the circuit. Since the pipe is buried in

the floor, the length is unknown, but if Assumption 4 is true, the length is given by

$$\ell_{r,j} = g_p A_{r,j} \quad (10)$$

where g_p is the common pipe length per area floor. Inserting Eq. (9) and (10) into (8) gives

$$q_j = A_p g_p \rho \frac{A_{r,j}}{\Delta t_{r,j}}. \quad (11)$$

According to Assumptions 4 and 2 the pipe area A_p , mass density of water ρ and pipe length factor g_p are common for all circuits, meaning that the flow in circuit q_j is proportional to the ratio $A_{r,j}/\Delta t_{r,j}$.

$$q_j \propto \frac{A_{r,j}}{\Delta t_{r,j}} = \alpha_j \quad (12)$$

2.5 Measuring the round trip time Δt_j

According to assumption 5, the room areas are assumed known, but the circulation time $\Delta t_{r,j}$ for circuit j is not, meaning it has to be measured. To measure the round trip time Δt_j of circuit j , time series measurements from the forward temperature T_F and individual return temperatures $T_{R,j}$ are used.

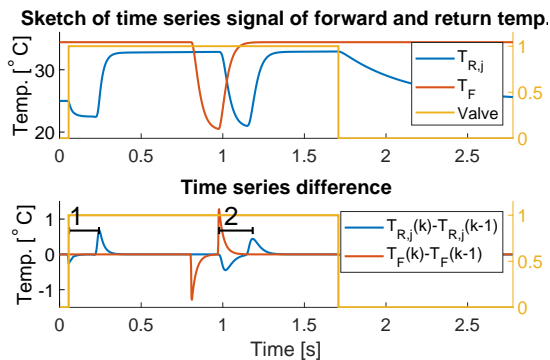


Fig. 3 – Shows a sketch of the measured forward and return temperature of a circuit. The figure presents two events that can be used for measuring the round trip time. The first (marked 1) is the time after a circuit opens. In this period old cooled water is replaced by fresh warm. The second event (marked 2) is caused by a large step on the forward temperature. Note that k indicates sample number.

Events, shown in Figure 3, with rapid changes in the forward temperature can be observed on both the forward and return temperature sensor. First on the forward temperature sensor, then later in a low pass filtered version on the return sensor. The challenge lies in figuring out when to start and stop the timer. It has been observed from measurements that the steepest gradient on the signal marks a sufficient and often clear point in the data; this claim is explained in more detail in Section 3.1. By taking the time series difference, the slope graph is obtained, and the round trip time is easily measured as the time distance between the two peaks.

2.6 Considerations on circulation time Δt_r

Having shown that the flow is proportional to room area over room circulation time, this section deals with the estimate of the circulation time. The simple expression in Eq. (11) is derived under the assumption that the circulation time under floor, denoted $\Delta t_{r,j}$, is measured. This is equivalent to measure from (1) to (2) in Fig. 1. In practice, however, it is the time from point (S) to (E), denoted Δt_j , which is measured. Eq. (13) shows the relation between the measured, Δt_j , and desired time, $\Delta t_{r,j}$:

$$\Delta t_j = \Delta t_{r,j} + 2\Delta t_{tr,j} \quad (13)$$

where Δt_{tr} is the transport time from the manifold to the floor. The time Δt_{tr} is scaled by two because the water has to be transported to and back from the floor. If the transport time is not considered, a significant bias is introduced. It is a weakness of the method that it is the round trip time, and not the time spent under the floor, that is measured. This said, it is possible to compensate for this bias by using information from the system. To obtain the corrected circulation time one has to obtain an estimate of the percentage share of the full pipe length placed under the floor, \mathcal{P}_r . The percentage share \mathcal{P}_r , seen in Eq. (14), is calculated using estimates on the length of the transport pipe $\hat{\ell}_{tr}$ and the length of pipe per square meter floor \bar{g}_p .

$$\begin{aligned} \hat{\Delta t}_{r,j} &= \Delta t_j \frac{\ell_{r,j}}{\ell_{r,j} + 2\hat{\ell}_{tr,j}} \\ &= \Delta t_j \frac{\bar{g}_p A_{r,j}}{\bar{g}_p A_{r,j} + 2\hat{\ell}_{tr}} = \Delta t_j \mathcal{P}_{r,j} \end{aligned} \quad (14)$$

This means that the estimate of the pipe length under the floor ℓ_r , is based on an assumption of a linear relationship between floor area and pipe length. The pipe density g_p is often between 3 and 6 m/m^2 . The transport length $\ell_{tr,j}$ can be estimated with some uncertainty, based on distance from room to manifold. Inserting Eq. (14) into (12) gives the corrected proportionality constant:

$$q_j \propto \frac{A_{r,j}}{\Delta t_j \frac{\bar{g}_p A_{r,j}}{\bar{g}_p A_{r,j} + 2\hat{\ell}_{tr}}} = \frac{A_{r,j} + \frac{2\hat{\ell}_{tr}}{\bar{g}_p}}{\Delta t_j} = \alpha_j \quad (15)$$

The updated expression seen in (15) is used to calculate the RHC coefficient α_j .

2.7 Simulation

To investigate the claim that the maximum slope measures the complete circulation time, a simulation of a simple floor heating system is implemented. As seen in Figure 4, the model consists of six parts. A room modelled as a first order system, a floor, a water pipe (under floor

and two transport sections), a piece of pipe placed in the heating room and a simple sensor model attached to this pipe. Note that indexes such as i and j refer to partitions of one pipe and not circuits, since the model is representative for all circuits.

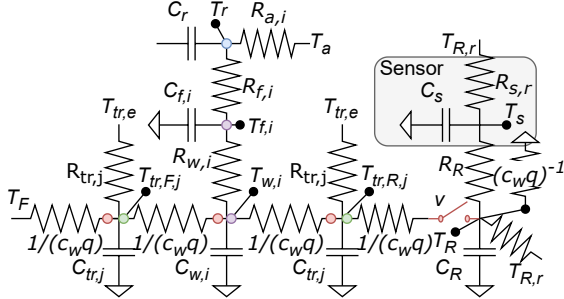


Fig. 4 – Shows the resistor-capacitor equivalent of the simulation model. The green dot indicates that this model section is repeated M_{part} times. The purple dot indicates that the section is repeated N_{part} times. The blue dot describes a summation point, where the heat contribution from all the floor parts are collected. The red dots indicate circuit breakers. If the binary valve indicator is 1 the circuit is closed and the water is flowing, and 0 stops the flow.

The model of the transport pipe (tr), for both directions are shown in Eq. (16a).

$$C_{\text{tr},\{\cdot\},j} \dot{T}_{\text{tr},\{\cdot\},j} = c_w q (T_{\text{tr},\{\cdot\},j-1} - T_{\text{tr},\{\cdot\},j}) v + \frac{1}{R_{\text{tr},i}} (T_{\text{tr},e} - T_{\text{tr},\{\cdot\},j}) \quad (16a)$$

with C being the heat capacity, T the temperature, q the nominal mass flow, $v \in \{0, 1\}$ the valve indicator variable and R the heat resistance. The placeholder $\{\cdot\}$ indicates that the equation is valid for both the *forward* (F) and *return* (R) pipe. This is the case since they are modelled as being equally long. The pipes have M_{part} partitions each, with $j \in \{1, \dots, M_{\text{part}}\}$. The equation consists of a term describing the water being transported within the pipe and one describing transport loss. Eq. (16b) describes the water in the pipe under the floor:

$$C_{w,i} \dot{T}_{w,i} = \frac{1}{R_{w,i}} (T_{f,i} - T_{w,i}) + c_w q (T_{w,i-1} - T_{w,i}) v \quad (16b)$$

Again a term describes the water transport and one describes the transfer of energy to the *floor* (f) slab. Note that losses to the ground or other rooms are not considered. There are N_{part} partitions, with $i \in \{1, \dots, N_{\text{part}}\}$. Eq. (16c) shows the equation for floor partition i . There is an equal number of floor and water pipe partitions, since they are paired together.

$$C_{f,i} \dot{T}_{f,i} = \frac{1}{R_{w,i}} (T_{w,i} - T_{f,i}) + \frac{1}{R_{f,i}} (T_{f,i} - T_r) \quad (16c)$$

The floor partition is nothing more than a capacitance and two resistances placed between the the pipe and room. Eq. (16d) describes a *room* (r) with an equal distributed air temperature.

$$C_r \dot{T}_r = \sum_{i=1}^N \frac{1}{R_{f,i}} (T_{f,i} - T_r) + \frac{1}{R_{a,i}} (T_a - T_{r,i}) \quad (16d)$$

The energy flow from the floor is the sum of the flow from each floor partition. The other term describes the heat loss to the environment. Eq. (16e) describes the part of the return pipe (R) placed in the heating room.

$$C_r \dot{T}_R = c_w q (T_{\text{tr},R,N_{\text{part}}} - T_R) v + \frac{1}{R_{R,r}} (T_{R,r} - T_R) + \frac{1}{R_R} (T_s - T_R) \quad (16e)$$

Eq. (16e) has three terms, the water flow, a small heat loss to the sensor and the loss to the heating room. Eq. (16f) describes the temperature sensor as a small first order capacity. The state T_s describes the measured value.

$$C_s \dot{T}_s = \frac{1}{R_{s,r}} (T_{R,r} - T_s) + \frac{1}{R_R} (T_R - T_s) \quad (16f)$$

$$T_{\text{tr},F,1} = T_F \quad T_r \in \mathbb{R} \quad \mathbf{T}_f \in \mathbb{R}^{N_{\text{part}}} \quad \mathbf{T}_w \in \mathbb{R}^{N_{\text{part}}}$$

The water pipe is divided into two *transport* (tr) sections and the part embedded in the floor. The floor and pipes are discretized along the length, which makes the model a high order system. The length of each partition ℓ_{part} in the floor and transport pipe is decided by a exchange percentage α_p , meaning a certain percentage of water needs to be exchanged at each sample.

$$\ell_{\text{part}} = \frac{q dt}{\rho_w \pi r_p^2 \alpha_p} \implies \ell_{dt} = \alpha_p \ell_{\text{part}} \quad (17)$$

where ℓ_{dt} is the distance the water travel each simulation sample period dt . To create a correlation between coefficients in the simulation, a number of relations can be formulated for heat capacities, $C_{\{\cdot\}}$, and resistances $R_{\{\cdot\}}$.

$$C_{w,i} = C_{\text{tr},\{\cdot\},j} = c_w \rho_w A_p \ell_{\text{part}} \quad (18)$$

$$C_R = c_w \rho_w A_p \ell_R \quad (19)$$

$$C_{f,i} = \frac{A_r g_f}{N_{\text{part}}} \quad C_r = V_r c_a \rho_a + A_r g_e \quad (20)$$

$$R_{w,i} = \frac{N_{\text{part}}}{2\pi r_p u_w g_p A_r} \quad R_{\text{tr},i} = \frac{1}{2\pi r_p u_{\text{tr}} \ell_{\text{part}}} \quad (21)$$

$$R_{R,r} = \frac{1}{2\pi r_p u_{R,r} \ell_R} \quad (22)$$

$$R_{a,i} = \frac{N_{\text{part}}}{u_a A_r} \quad R_{f,i} = \frac{N_{\text{part}}}{u_f A_r} \quad (23)$$

$$R_R = \frac{1}{U_R} \quad R_{s,r} = \frac{1}{U_{s,r}} \quad (24)$$

$$q = g_q A_r \quad (25)$$

with A_p being the cross area of the pipe and ρ , c the density and specific heat capacity, respectively. Volumes are denoted as V . The heat capacity per square meter floor is given as g_f . The heat conduction per square meter is u and heat conduction is U . The ratio between floor area and wall capacity and flow is given by g_e and g_q , respectively. The model can then be summed up as an switched-input linear model. The state space version is seen in (26):

$$\mathbf{C}\dot{\mathbf{T}} = v\mathbf{A}_{\text{on}}\mathbf{T} + (v-1)\mathbf{A}_{\text{off}}\mathbf{T} + v\mathbf{B}T_F + \mathbf{E}d \quad (26)$$

where \mathbf{A} , \mathbf{B} , \mathbf{C} and \mathbf{E} are matrices and \mathbf{T} a vector of temperatures. The model is simulated with a time period of dt using first order Euler integration.

$$\begin{aligned} \mathbf{T}(k+1) &= [\mathbf{I} + v(k)\mathbf{A}_{\text{on}}dt + (v(k)-1)\mathbf{A}_{\text{off}}dt] \\ &\mathbf{T}(k) + v(k)dt\mathbf{B}T_F(k) + dt\mathbf{E}d(k) \end{aligned} \quad (27)$$

2.8 Experiment in test house

The test house used in this project has a flow-meter on the common circuit of the FH system. This flow-meter is used to establish a baseline flow distribution. To obtain the distribution, the flow is measured with only one circuit open. This is done for all circuits. Note, the distribution obtained from this approach does not account for any saturation effects on the circulation pump occurring at high flow rates.

To obtain the round trip times Δt_j used for Eq. (15), all circuits are opened. Then a step in the forward temperature is performed by turning of the heat source while circulating the water. In this particular case the heat pump turned off periodically. This is illustrated as event two in Fig. 3 and seen in Fig 5.b. The data from the return sensors is sampled with a period of 20 seconds and low-pass filtered to reduce noise and quantization effects. Multiple samples are carried out and averaged. In practice the experiment can be carried out without forcing the circuits open.

3. Results

This section presents the results from the simulation based sensitivity analysis and the experiment on the inhabited test house.

3.1 Simulation results

In Sec. 2.5 it is claimed that round-trip time can be measured using the return sensors. In this section, the simulation from Sec. 2.7 is used to investigate whether this is consistent under varying conditions and configurations.

Tab. 1 – The distribution of random parameters

Parameter	Distribution	Unit
A_r	$\mathcal{U}(5, 30)$	$[m^2]$
g_q	$\mathcal{U}(0.002, 0.005)$	$[kg/(m^2s)]$
g_f	$\mathcal{U}(24000, 36000)$	$[J/(m^2K)]$
g_e	$\mathcal{U}(12000, 17000)$	$[J/(m^2K)]$
g_a	$\mathcal{U}(0.3, 1)$	$[-]$
r_p	$\mathcal{U}(0.01, 0.02)$	$[m]$
u_a	$\mathcal{U}(0.45, 0.55)$	$[W/(m^2K)]$
u_f	$\mathcal{U}(3.5, 4.5)$	$[W/(m^2K)]$
u_w	$\mathcal{U}(6, 12)$	$[W/(m^2K)]$
u_{tr}	$\mathcal{U}(2, 4)$	$[W/(m^2K)]$
$u_{R,r}$	$\mathcal{U}(0.05, 0.15)$	$[W/(m^2K)]$
U_R	$\mathcal{U}(0.5, 0.5)$	$[W/K]$
$U_{s,r}$	$\mathcal{U}(0.05, 0.15)$	$[W/K]$
ℓ_{tr}	$\mathcal{U}(3, 25)$	$[m]$
C_s	$\mathcal{U}(80, 120)$	$[J/K]$
\mathcal{P}_p	$\mathcal{U}(0.5, 0.5)$	$[-]$

The analysis is performed by repeating a 10 room simulation, supplied with randomly drawn coefficients, 100 times. The coefficients are distributed according to Tab. 1 where \mathcal{U} denotes the uniform distribution. The pipe distribution g_p , follows Assumption 4. Fig. 5 shows the transient response from the simulation compared with the measured one.

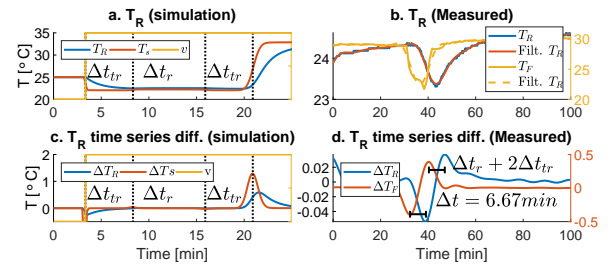


Fig. 5 – Column one: shows an example of the simulated transient response and time series diff. for the simulation. Column two: shows one of the measured values. Note that $\Delta T_R = T_R(k) - T_R(k-1)$.

The simulation allows us to investigate otherwise inaccessible states such as transport time Δt_{tr} and the actual water temperature T_R . As mentioned in Sec. 2.5, the peak for ΔT_R , seen in Fig. 5.c, exactly measures the total round trip time. We think this is the case, since this is the time where the new front of warm water arrives at the sensor. Further, it can be seen that the measured value T_s has a slower time constant, since the heat needs to propagate through the pipe. To measure the performance the root mean square error seen in (28), is computed for the difference between the actual flow distribution $\mathcal{P}_q \in \mathbb{R}^N$ and the particular flow distribution estimates $\mathcal{P}_{x,j}$ with $x \in \alpha, A_r$. The subscript α indicates that the distribution is based on Eq. (15), and A_r that it is

based purely on area distribution.

$$RMSE_{E_x} = \frac{1}{N} \sum_{j=1}^N (\mathcal{P}_{q,j} - \hat{\mathcal{P}}_{x,j}) \quad (28)$$

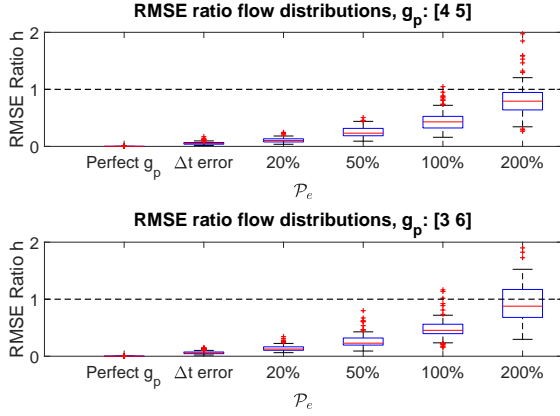


Fig. 6 – Upper and lower show the RMSE ratio of the test performed with the pipe density g_p drawn uniformly between 4 and 5 and 3 to 6 m/m^2 , respectively. The x-axis shows the results with increased error on the transport pipe estimate. The first entry contains the results using perfect information. The second shows the results where only the error from measuring the round-trip time affects the result. \mathcal{P}_e is the percentage error.

To quantify the results, the root mean square error calculated from the simulations are formulated as a ratio h seen in Eq. (29).

$$h = \frac{RMSE_{E_\alpha}}{RMSE_{A_r}} \quad (29)$$

This ratio allows us to evaluate whether the overall distribution improved. If h is zero, it means that the fit is perfect, and if it is greater than one, it would be better to distribute based on area alone. The estimates for the flow distribution, $\mathcal{P}_{\alpha,j}$, is calculated using the normalized version of (15) with $\bar{g}_p = 4.5$ and $\hat{\ell}_{tr}$ as the real transport length plus estimation error:

$$\hat{\ell}_{tr} = \ell_{tr} + e_{tr} \quad (30)$$

The error is correlated with the actual length of the transport pipe and normally distributed according to the following 3σ rule.

$$e_{tr} \sim \mathcal{N}(0, (1/3\mathcal{P}_e\ell_{tr})^2) \quad (31)$$

where $1/3\mathcal{P}_e\ell_{tr}$ is the standard deviation of the error of the one-way transport distance, meaning that 99% of the errors are within plus/minus this range. Figure 6 and 7 show the results of the simulations. As can be seen in Figure 6, it is important to have a good estimate of the length of the transport pipe, since it has a large effect on the quality of the estimate. The outliers, seen with red crosses, have been related to bad measurements where the wrong peak is obtained.

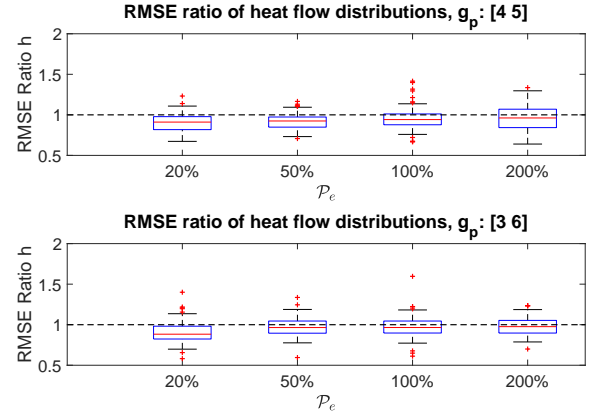


Fig. 7 – Sums up the results for the calculated heat distributions. The figure has the same structure as Fig. 6. The RMSE resulting from using the RHC in Eq. (4) is divided by the RMSE from Eq. (32).

The heat distributions, defined as the percentage share of accumulated heat consumption, are also calculated from the simulations. The heat distribution is based on the RHC in Eq. (4) and compared with Eq. (32) taken from [6].

$$\beta_{A_{r,j}}(t) = A_{r,j} \frac{T_F(t) - T_{R,j}(t)}{\ln \left(\frac{T_F(t) - T_{r,j}(t)}{T_{R,j}(t) - T_{r,j}(t)} \right)} \quad (32)$$

This RHC also uses the return temperature together with the room temperature $T_{r,j}$ and floor area over the circuit. The RHC in Eq. (32) assumes that the specific heat conduction from water to room is the same for all rooms. The final heat distribution is obtained by integrating the RHC using Eq. (7). As in the case with pipe density, the specific heat conductance's in the floor are varied with each simulation, but kept constant between rooms in any given simulation. This is done to avoid punishing the method based on Eq. (32) unnecessarily. Considering the heat distribution the improvement is not that clear. It has to be mentioned that real floors do not have equal resistance, due to varying floor types and the effects caused by the interior of the room.

3.2 Demo house comparison

To collect evidence for or against the ability of the method to estimate the flow distribution in real houses, the method was carried out on a test house having a flow meter on the common pipe of the FH system. The measurement results of round-trip time Δt_r are seen in Tab. 3. Two measurements are made and the average value is used. Note that the times differ quite significantly between the two tests, and the reason for this is unexplained. It is worth noting, though, that if the values are plotted, the pattern is preserved. Besides the measured times, the actual measured flow for each circuit is shown in liters per hour. The areas and assumed transport lengths are presented too. Figure 8 shows the results of the estimated flow distribution. As can be seen, 12

out of 15 circuits improved when compared to the measured distribution.

Tab. 2 – Shows the RMSE and *mean absolute error* (MAE) of the estimates for the nominal flow distribution based on floor area and Eq. 15

Measure	A_r	$\frac{A_r}{\Delta t}$	Ratio h
RMSE	0.014	0.0093	0.62
MAE	0.012	0.0077	0.63

Tab. 3 – Results for room 1-15

Room	1	2	3	4	5	6	7	8
$q[l/h]$	173	135	87	154	158	184	119	132
$\Delta t_{r,j}^1[s]$	460	500	440	480	420	420	280	480
$\Delta t_{r,j}^2[s]$	420	440	380	480	340	340	240	440
$A_{r,j}[m^2]$	12.7	9.2	3.6	9.5	9.3	9.6	4.8	9.5
$\hat{\ell}_{tr,j}[m]$	8	5.5	7	1.5	3	3	1.5	5.5

Room	9	10	11	12	13	14	15
$q[l/h]$	126	184	150	140	165	156	95
$\Delta t_{r,j}^1[s]$	440	520	520	480	360	460	300
$\Delta t_{r,j}^2[s]$	340	500	460	400	300	360	280
$A_{r,j}[m^2]$	9.5	15	14.6	7.7	9.6	13	5.5
$\hat{\ell}_{tr,j}[m]$	5.5	11.5	2.5	8.5	3	2	2

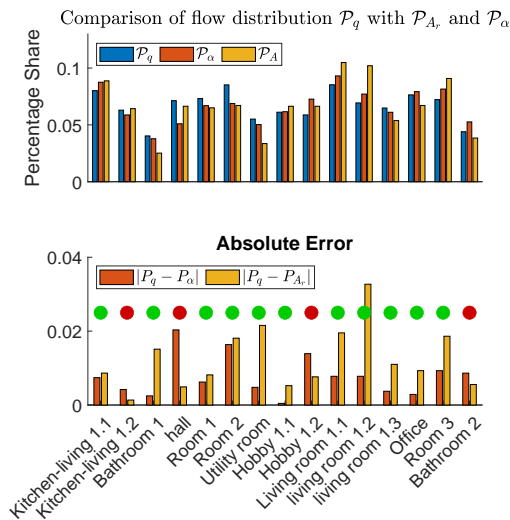


Fig. 8 – Upper: Comparison of real percentage share of flow with estimate based on α and A_r . Lower: difference for each room plus improvement indicator.

4. Conclusion

In this work we investigated the use of retrofitted sensors on the return pipes to estimate the flow distribution in a FH system. Simulation and experimental results suggest that it is possible to observe round-trip time in the data, and the flow distribution resulting therefrom is better than the one merely based on floor area distribution. The method improved the estimate in a test house by 38%. Work to be done, is to carry out a statistic, which either supports or disproves the result presented in this text. The results also suggest that measuring the temperature in the pipe could improve the results substantially.

The datasets generated during and/or analysed during the current study are available in the git repository, <https://gitlab.com/Thorsteinsson/clima-2022.git>.

References

- [1] Danish Energy Agency, “Data, tabeller, statistikker og kort Energistatistik 2019,” da, Danish Energy Agency, Tech. Rep., ISSN: 0906-4699 year: 2019, p. 60. [Online]. Available: https://ens.dk/sites/ens.dk/files/Statistik/energistatistik2019_dk-webtilg.pdf (visited on 05/07/2021).
- [2] Statistics Denmark, *Boligbestanden*, da, 2021. [Online]. Available: <https://www.dst.dk/da/Statistik/emner/borgere/boligforhold/boligbestanden> (visited on 11/25/2021).
- [3] P. D. Andersen, M. J. Jiménez, H. Madsen, and C. Rode, “Characterization of heat dynamics of an arctic low-energy house with floor heating,” en, *Building Simulation*, vol. 7, no. 6, pp. 595–614, Dec. 2014, ISSN: 1996-8744. DOI: 10.1007/s12273-014-0185-4.
- [4] I. Hazyuk, C. Ghiaus, and D. Penhouet, “Optimal temperature control of intermittently heated buildings using Model Predictive Control: Part I – Building modeling,” en, *Building and Environment*, vol. 51, pp. 379–387, May 2012, ISSN: 0360-1323. DOI: 10.1016/j.buildenv.2011.11.009.
- [5] P. Radecki and B. Hency, “Online Model Estimation for Predictive Thermal Control of Buildings,” *IEEE Transactions on Control Systems Technology*, vol. 25, no. 4, pp. 1414–1422, Jul. 2017, Conference Name: IEEE Transactions on Control Systems Technology, ISSN: 1558-0865. DOI: 10.1109/TCST.2016.2587737.
- [6] J. Ploennigs, A. Ahmed, B. Hensel, P. Stack, and K. Menzel, “Virtual sensors for estimation of energy consumption and thermal comfort in buildings with underfloor heating,” en, *Advanced Engineering Informatics*, Special Section: Advances and Challenges in Computing in Civil and Building Engineering, vol. 25, no. 4, pp. 688–698, Oct. 2011, ISSN: 1474-0346. DOI: 10.1016/j.aei.2011.07.004.
- [7] T. M. Kull, M. Thalfeldt, and J. Kurnitski, “Modelling of Wax Actuators in Underfloor Heating Manifolds,” en, *E3S Web of Conferences*, vol. 246, p. 11 009, 2021, Publisher: EDP Sciences, ISSN: 2267-1242. DOI: 10.1051/e3sconf/202124611009.